

## **CO-REGISTRATION OF LARGE VOLUME LASER SCANNER POINT CLOUDS: THE PINCHANGO ALTO (PERU) DATA SET**

Internal Technical Report

by

Devrim Akca

Group of Photogrammetry and Remote Sensing (P+F), ETH Zurich

[www.photogrammetry.ethz.ch](http://www.photogrammetry.ethz.ch)

Presented to

Prof. Dr. Armin Gruen

Prepared for the project

3D Modeling of the pre-Inkaic site Pinchango Alto, Peru

a cooperation of

Group of Photogrammetry and Remote Sensing of ETH Zurich

and

German Institute of Archaeology (KAVA, Bonn, Germany)

Swiss Federal Institute of Technology (ETH) Zurich

Institute of Geodesy and Photogrammetry

ETH-Hoenggerberg, CH-8093 Zurich

July 2005

## TABLE OF CONTENTS

List of figures .....	3
List of tables .....	3
1. Introduction .....	4
2. Least Squares 3D Surface Matching (LS3D) .....	6
2.1. The basic estimation model .....	6
2.2. Error detection and execution aspects .....	8
2.3. Fast correspondence computation with boxing structure .....	9
2.4. Simultaneous multi-subpatch matching .....	10
3. Registration of Pinchango Alto Laser Scans .....	10
3.1. The scanner .....	10
3.2. The scanning campaign .....	11
3.3. Pairwise registration with the LS3D surface matcher .....	12
3.4. Global registration .....	14
4. Surface Mesh generation and Modeling .....	14
4.1. Modeling with Geomagic Studio 6 .....	17
4.2. Modeling with ArcGIS 9 .....	18
5. Conclusions .....	19
Acknowledgements .....	20
References .....	20

## LIST OF FIGURES

1	Location of Pinchango Alto, Peru .....	4
2	Panorama of Pinchango Alto site .....	5
3	The Riegl LMS-Z420i scanner is at the site .....	11
4	Area1 and Area2 .....	11
5	Day by day coverage of the site .....	12
6	Intensity image of a nearly 90 degree subpart of scan #8 .....	13
7	Top view of the point cloud of Figure 6 in 3D .....	13
8	Non-static objects on the site .....	16
9	Holes due to missing data .....	16
10	Shaded view of the generated model using Geomagic Studio 6 .....	17
11	Shaded view of the generated model using ArcGIS 9 .....	18
12	The same zoom in area of the generated surface model using Geomagic Studio (a) and ArcGIS (b) .....	19

## LIST OF TABLES

1	Numerical results of the LS3D matching .....	15
---	--	----

## 1. Introduction

Pinchango Alto is the largest Late Intermediate Period (LIP, AD 1000–1400) site in the Palpa area (Fig. 1). The site is located about 3 km north of the modern town of Palpa (Peru) on an elongated rocky spur on the western slope of Cerro Pinchango. The central part of the site covers an area of roughly 3 ha on the flat ridge of the spur (Fig. 2). The ruins are composed of partially collapsed double-faced walls built of unworked stones, today preserved to a maximum height of about 1.5 m. These walls once formed agglutinated rooms, enclosures, corridors, and several large plazas. Due to its hidden location, the site has suffered less looting than most other sites in the region of Palpa and Nasca (Eisenbeiss et al., 2005).

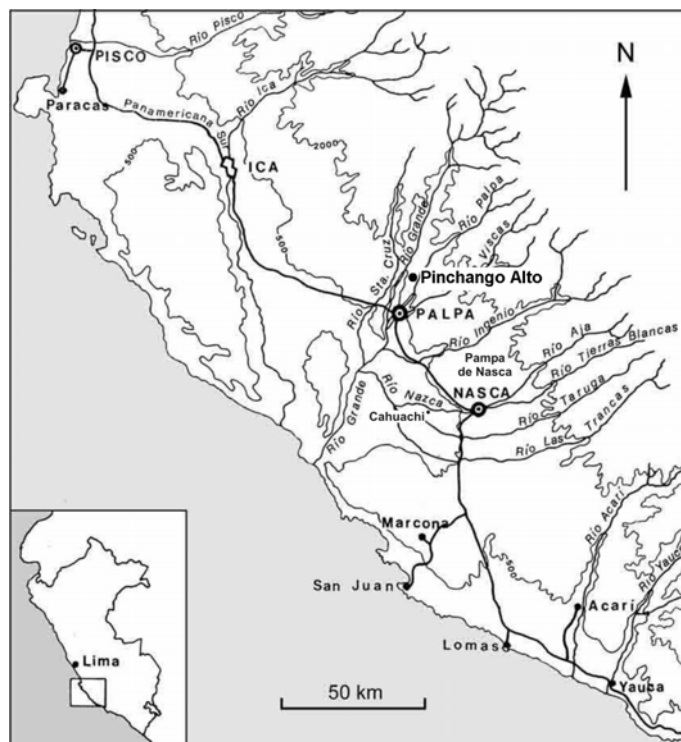


Figure 1. Location of Pinchango Alto, Peru.

The site was documented under the framework of a research program called NTG (“New methods and technologies in the humanities”) funded by the German Ministry of Education and Research (BMBF, Bonn). The project aims to investigate the applicability of the modern surveying techniques to archaeological documentation studies. Two systems, a terrestrial laser scanner and a UAV (Unmanned Aerial Vehicle) system, were employed during the September 2004 field campaign. The field work was conducted in cooperation with Riegl Laser Measurement Systems (Austria), Helicam (Switzerland), the German Institute of Archaeology, Commission for General and Comparative Archaeology (KAVA) in Bonn (Germany) and the Group of Photogrammetry and Remote Sensing of ETH Zurich (Switzerland). Further information can be found on the project webpage: <http://www.photogrammetry.ethz.ch/research/pinchango> .

A model helicopter carrying a Canon EOS-D60 CMOS camera was used to acquire in a single day a series of aerial images. The photogrammetric processing of those images was carried out at ETH Zurich. The results have been presented in Eisenbeiss et al. (2005).



Figure 2. Panorama of Pinchango Alto site.

A Riegl LMS-Z420i laser scanner kindly provided by Riegl GmbH, Horn (Austria), was used to scan the whole area in 5 days. For registration of the point clouds retro reflective cylindrical targets (Standard cylinders by Riegl GmbH) were used. The coordinates of the targets were measured with RTK-GPS.

Terrestrial laser scanning companies (e.g. Z+F, Leica, Riegl) commonly use special kind of targets for the registration of point clouds. However such a strategy has several deficiencies with respect to fieldwork time, labour, personnel and equipment costs, and accuracy. In a recent study Sternberg et al. (2004) reported that registration and geodetic measurement parts comprise 10-20% of the whole project time. In another study a collapsed 1000-car parking garage was documented in order to assess the damage and structural soundness of the structure. The scanning took 3 days, while the conventional survey of the control points required 2 days (Greaves, 2005). In our work at Pinchango Alto 2 persons set the targets to the field and measured with RTK-GPS in 1½ days.

Not only fieldwork time but also accuracy is another important concern. The target based registration methods cannot exploit the full accuracy potential of the data. The geodetic measurement naturally introduces some error, which might exceed the internal error of the scanner instrument. In addition the targets must be kept stable during the whole scanning campaign. This might be inconvenient with the scanning works more than one day.

Surface based registration techniques stand as efficient and versatile alternative to the target based techniques. They simply bring the strenuous additional fieldwork of the registration task to the computer in office while optimizing the project cost and duration and achieving a better accuracy.

Recently we have developed an algorithm for the least squares matching of overlapping 3D surfaces (Gruen and Akca, 2004; Gruen and Akca, 2005b). It estimates the transformation parameters between two or more fully 3D surfaces, using the Generalized Gauss-Markoff model, minimizing the sum of squares of the Euclidean distances between the surfaces. This formulation gives the opportunity of matching arbitrarily oriented 3D surfaces simultaneously, without using explicit tie points. Our mathematical model is a generalization of the least squares image matching method, in particular the method given by Gruen (1985). We gave further extensions of the basic model: simultaneous matching of multi sub-surface patches, and matching of surface geometry and its attribute information, e.g. reflectance, color, temperature, etc. under a combined estimation model (Gruen and Akca, 2005a).

The Pinchango Alto laser scanning data set was registered using our in-house surface matching method. The Pinchango Alto data set is an extreme case due to huge data volume (totally 144 million points) and large occlusions. This report presents the results and the gained experiences. The outline of the report is as follow. The details of the mathematical modeling of our surface matching method and the execution aspects are explained in the following section. The numerical results of the matching are given in the third section. The mesh generation was performed using two different commercial software packages, i.e. Geomagic Studio 6 (Raindrop Geomagic) and ArcGIS 9 (ESRI). The result of the modeling part is given in the fourth section.

## 2. Least Squares 3D Surface Matching (LS3D)

### 2.1. The basic estimation model

Assume that two different partial surfaces of the same object are digitized/sampled point by point, at different times (temporally) or from different viewpoints (spatially).  $f(x, y, z)$  and  $g(x, y, z)$  are conjugate regions of the object in the *left* and *right* surfaces respectively. In other words  $f(x, y, z)$  and  $g(x, y, z)$  are discrete 3D representations of the *template* and *search* surfaces. The problem statement is estimating the final location, orientation and shape of the search surface  $g(x, y, z)$ , which satisfies minimum condition of Least Squares Matching with respect to the template  $f(x, y, z)$ . In an ideal situation one would have

$$f(x, y, z) = g(x, y, z) \quad (1)$$

Taking into account the noise and assuming that the template noise is independent of the search noise, Equation (1) becomes

$$f(x, y, z) - e(x, y, z) = g(x, y, z) \quad (2)$$

where  $e(x, y, z)$  is a true error vector. Equation (2) are observation equations, which functionally relate the observations  $f(x, y, z)$  to the parameters of  $g(x, y, z)$ . The matching is achieved by least squares minimization of a goal function, which represents the sum of squares of the Euclidean distances between the surfaces. The final location is estimated with respect to an initial position of  $g(x, y, z)$ , the approximation of the conjugate search surface  $g^o(x, y, z)$ .

To express the geometric relationship between the conjugate surface patches, a 7-parameter 3D similarity transformation is used:

$$[x \ y \ z]^T = [t_x \ t_y \ t_z]^T + m \mathbf{R} [x_0 \ y_0 \ z_0]^T \quad (3)$$

where  $\mathbf{R} = \mathbf{R}(\omega, \phi, \kappa)$  is the orthogonal rotation matrix,  $[t_x \ t_y \ t_z]^T$  is the translation vector, and  $m$  is the uniform scale factor. This parameter space can be extended or reduced, as the situation demands it.

In order to perform least squares estimation, Equation (2) must be linearized by Taylor expansion.

$$f(x, y, z) - e(x, y, z) = g^o(x, y, z) + \frac{\partial g^o(x, y, z)}{\partial x} dx + \frac{\partial g^o(x, y, z)}{\partial y} dy + \frac{\partial g^o(x, y, z)}{\partial z} dz \quad (4)$$

with

$$dx = \frac{\partial x}{\partial p_i} dp_i, \quad dy = \frac{\partial y}{\partial p_i} dp_i, \quad dz = \frac{\partial z}{\partial p_i} dp_i \quad (5)$$

where  $p_i \in \{t_x, t_y, t_z, m, \omega, \phi, \kappa\}$  is the  $i$ -th transformation parameter in Equation (3). Differentiation of Equation (3) gives:

$$\begin{aligned} dx &= dt_x + a_{10} dm + a_{11} d\omega + a_{12} d\phi + a_{13} d\kappa \\ dy &= dt_y + a_{20} dm + a_{21} d\omega + a_{22} d\phi + a_{23} d\kappa \\ dz &= dt_z + a_{30} dm + a_{31} d\omega + a_{32} d\phi + a_{33} d\kappa \end{aligned} \quad (6)$$

where  $a_{ij}$  are the coefficient terms, whose expansions are trivial. Using the following notation

$$g_x = \frac{\partial g^o(x, y, z)}{\partial x}, \quad g_y = \frac{\partial g^o(x, y, z)}{\partial y}, \quad g_z = \frac{\partial g^o(x, y, z)}{\partial z} \quad (7)$$

and substituting Equations (6), Equation (4) results in the following:

$$\begin{aligned} -e(x, y, z) &= g_x dt_x + g_y dt_y + g_z dt_z \\ &\quad + (g_x a_{10} + g_y a_{20} + g_z a_{30}) dm \\ &\quad + (g_x a_{11} + g_y a_{21} + g_z a_{31}) d\omega \\ &\quad + (g_x a_{12} + g_y a_{22} + g_z a_{32}) d\phi \\ &\quad + (g_x a_{13} + g_y a_{23} + g_z a_{33}) d\kappa \\ &\quad - (f(x, y, z) - g^o(x, y, z)) \end{aligned} \quad (8)$$

In the context of the Gauss-Markoff model, each observation is related to a linear combination of the parameters, which are variables of a deterministic unknown function. The terms  $\{g_x, g_y, g_z\}$  are numeric first derivatives of this function  $g(x, y, z)$ . Equation (8) gives in matrix notation

$$-e = \mathbf{A}\mathbf{x} - \mathbf{l}, \quad \mathbf{P} \quad (9)$$

where  $\mathbf{A}$  is the design matrix,  $\mathbf{x}^T = [dt_x \ dt_y \ dt_z \ dm \ d\omega \ d\phi \ d\kappa]$  is the parameter vector, and  $\mathbf{l} = f(x, y, z) - g^o(x, y, z)$  is the discrepancy vector that consists of the Euclidean distances between the template and correspondent search surface elements. The template surface elements are approximated by the data points, on the other hand the search surface elements are represented in two different kind of piecewise surface forms (planar and bi-linear) optionally. In general both surfaces can be represented in any kind of piecewise form.

With the statistical expectation operator  $E\{\}$  and the assumptions  $E\{\mathbf{e}\} = \mathbf{0}$ ,  $E\{\mathbf{e}\mathbf{e}^T\} = \sigma_o^2 \mathbf{P}_I$  Equation (9) is a Gauss-Markoff estimation model, where  $\mathbf{P} = \mathbf{P}_I$  is a *a priori* weight matrix.

The unknown transformation parameters are treated as stochastic quantities using proper *a priori* weights. This extension gives advantages of control over the estimating parameters. We introduce the additional observation equations on the system parameters as

$$-\mathbf{e}_b = \mathbf{I}\mathbf{x} - \mathbf{I}_b, \quad \mathbf{P}_b \quad (10)$$

where  $\mathbf{I}$  is the identity matrix,  $\mathbf{I}_b$  is the (fictitious) observation vector for the system parameters, and  $\mathbf{P}_b$  is the associated weight coefficient matrix. The least squares solution of the joint system Equations (9) and (10) gives as the Generalized Gauss-Markoff model the unbiased minimum variance estimation for the parameters

$$\hat{\mathbf{x}} = (\mathbf{A}^T \mathbf{P} \mathbf{A} + \mathbf{P}_b)^{-1} (\mathbf{A}^T \mathbf{P} \mathbf{I} + \mathbf{P}_b \mathbf{I}_b) \quad (11)$$

$$\hat{\sigma}_o^2 = (\mathbf{v}^T \mathbf{P} \mathbf{v} + \mathbf{v}_b^T \mathbf{P}_b \mathbf{v}_b) / r \quad (12)$$

$$\mathbf{v} = \mathbf{A}\hat{\mathbf{x}} - \mathbf{I} \quad (13)$$

$$\mathbf{v}_b = \mathbf{I}\hat{\mathbf{x}} - \mathbf{I}_b \quad (14)$$

$\hat{\mathbf{x}}$  : solution vector

$\hat{\sigma}_o^2$  : variance factor

$\mathbf{v}$  : residuals vector for surface observations

$\mathbf{v}_b$  : residuals vector for parameter observations

where  $\hat{\cdot}$  stands for the Least Squares Estimator, and  $r$  is the redundancy. Since the functional model is non-linear, the solution is obtained iteratively. In the first iteration the initial approximations for the parameters must be provided. After the solution vector (Equation 11) is solved, the search surface  $g^o(x, y, z)$  is transformed to a new state using the updated set of transformation parameters, and the design matrix  $\mathbf{A}$  and the discrepancies vector  $\mathbf{I}$  are re-evaluated. The iteration stops if each element of the alteration vector  $\hat{\mathbf{x}}$  in Equation (11) falls below a certain limit:  $|dp_j| < c_i$ .

The numerical derivative terms  $\{g_x, g_y, g_z\}$  are defined as local surface normals  $\mathbf{n}$ . Their calculation depends on the analytical representation of the search surface elements. Two first degree  $C^0$  continuous surface representations are implemented: triangle mesh form, which gives planar surface elements, and optionally grid mesh form, which gives bi-linear surface elements. The derivative terms are given as  $x$ - $y$ - $z$  components of the local normal vectors:  $[g_x \ g_y \ g_z]^T = \mathbf{n} = [n_x \ n_y \ n_z]^T$ . For the details of the method we refer to (Gruen and Akca, 2005b).

## 2.2. Error detection and execution aspects

The standard deviations of the estimated transformation parameters and the correlations between themselves may give useful information concerning the stability of the system and quality of the data content (Gruen, 1985):

$$\hat{\sigma}_p = \hat{\sigma}_o \sqrt{q_{pp}}, \quad q_{pp} \in \mathbf{Q}_{xx} = (\mathbf{A}^T \mathbf{P} \mathbf{A} + \mathbf{P}_b)^{-1} \quad (15)$$

where  $\mathbf{Q}_{xx}$  is the cofactor matrix for the estimated parameters.

Detection of false correspondences with respect to the outliers and occlusions is a crucial part of every surface matching method. We use the following strategies in order to localize and eliminate the outliers and the occluded parts.

A median type of filtering is applied prior to the matching. For each point the distances between the central point and its 8-neighbourhood points are calculated. If some of those 8 distance values are much greater than the average point density, the central point is likely to be an erroneous point on a poorly reflecting surface (e.g. window or glass) or a range artifact due to surface discontinuity (e.g. points on the object silhouette). The central point is discarded according to the number of distances  $n$ , which are greater than a given distance threshold.

In the course of iterations a simple weighting scheme adapted from Robust Estimation Methods is used:

$$(\mathbf{P})_{ii} = \begin{cases} 1 & \text{if } |(\mathbf{v})_i| < K\sigma_o \\ 0 & \text{else} \end{cases} \quad (16)$$

In our experiments  $K$  is selected as  $>10$ , since it is aimed to suppress only the large outliers. It can be changed according to a given confidence level. Finally, we reject the correspondences containing points on the mesh boundaries. Because of the high redundancy of a typical data set, a certain amount of occlusions and/or smaller outliers do not have significant effect on the estimated parameters.

The convergence behaviour of the proposed method basically depends on the quality of the initial approximations and quality of the data content. For a good data configuration case it usually achieves the solution after 5 or 6 iterations.

Two first degree  $C^0$  continuous surface representations are implemented. In the case of multi-resolution data sets, in which point densities are significantly different on the template and search surfaces, higher degree  $C^1$  continuous composite surface representations, e.g. bi-cubic Hermit surface, should give better results, of course increasing the computational expense.

### 2.3. Fast correspondence computation with boxing structure

The computational effort increases with the number of points in the matching process. The main portion of the computational complexity is to search the corresponding elements of the template surface on the search surface, whereas the parameter estimation part is a small system, and can quickly be solved using Cholesky decomposition followed by back-substitution. Searching the correspondence is guided by an efficient boxing structure (Chetverikov, 1991), which partitions the search space into cuboids. For a given surface element, the correspondence is searched only in the box containing this element and in the adjacent boxes. In the original publication (Chetverikov, 1991) it was given for 2D point sets. We straightforwardly extend it to the 3D case. For the implementation details we refer to (Akca and Gruen, 2005). The access procedure requires  $O(q)$  operations, where  $q$  is the average number of points in the box. It is easy to implement and time-effective for accessing the data.

In our implementation, the correspondence is searched in the boxing structure during the first few iterations, and in the meantime its evolution is tracked across the iterations. Afterwards the searching process is carried out only in an adaptive local neighborhood according to the previous position and change of correspondence. In any step of the iteration, if the change of correspondence for a surface element exceeds a limit value, or oscillates, the search procedure for this element is returned to the boxing structure again.

#### 2.4. Simultaneous multi-subpatch matching

The basic estimation model can be implemented in a multi-patch mode, that is the simultaneous matching of two or more search surfaces  $g_i(x, y, z)$ ,  $i=1, \dots, k$  to one template  $f(x, y, z)$ .

$$- \mathbf{e}_i = \mathbf{A}_i \mathbf{x}_i - \mathbf{l}_i, \quad \mathbf{P}_i \quad (17)$$

Since the parameter vectors  $\mathbf{x}_1, \dots, \mathbf{x}_k$  do not have any joint components, the sub-systems of Equation (17) are orthogonal to each other. In the presence of auxiliary information those sets of equations could be connected via functional constraints, e.g. as in the Geometrically Constrained Multiphoto Matching (Gruen, 1985; Gruen and Baltsavias, 1988) or via appropriate formulation of multiple (>2) overlap conditions.

An ordinary point cloud includes enormously redundant information. A straightforward way to register such two point clouds could be matching of the whole overlapping areas. This is computationally expensive. We propose multi-subpatch mode as a further extension to the basic model, which is capable of simultaneous matching of sub-surface patches, which are interactively selected in cooperative surface areas. They are joined to the system by the same 3D transformation parameters. This leads to the observation equations

$$- \mathbf{e}_i = \mathbf{A}_i \mathbf{x} - \mathbf{l}_i, \quad \mathbf{P}_i \quad (18)$$

with  $i=1, \dots, k$  subpatches. They can be combined as in Equation (9), since the common parameter vector  $\mathbf{x}$  joints them to each other. The individual subpatches may not include sufficient information for the matching of whole surfaces, but together they provide a computationally effective solution, since they consist of only relevant information rather than using the full data set.

### 3. Registration of Pinchango Alto Laser Scans

#### 3.1. The scanner

The Riegl LMS-Z420i scanner (Fig. 3) was mainly chosen for its long scanning range of 800 m and the combination with a digital still-video camera. Its accuracy is of  $\pm 10$  mm (single shot) and  $\pm 5$  mm (averaged) with a beam divergence of 0.25 mrad (25 mm spot size @100m). Further features include: a measurement rate of up to 8000 pts/sec, a field of view of up to  $80^\circ \times 360^\circ$ , a digital camera Nikon D100 (6 megapixel), and a TCP/IP data interface allowing wireless data transmission operated by any standard PC or Notebook. The system is fully portable and robust. Further information can be found on the webpage of the scanner (Riegl, 2005)



Figure 3. The Riegl LMS-Z420i scanner is at the site.

### 3.2. The scanning campaign

The scanning campaign had been completed in 5 days of fieldwork. The site is around 300x150 meters in size. The whole area was covered with 61 scans, only 57 of which were registered. The remaining 4 scans were not used, since they cover the southern cliff part of the site which is not directly of interest, and due to insufficient overlapping with scans of the main area.

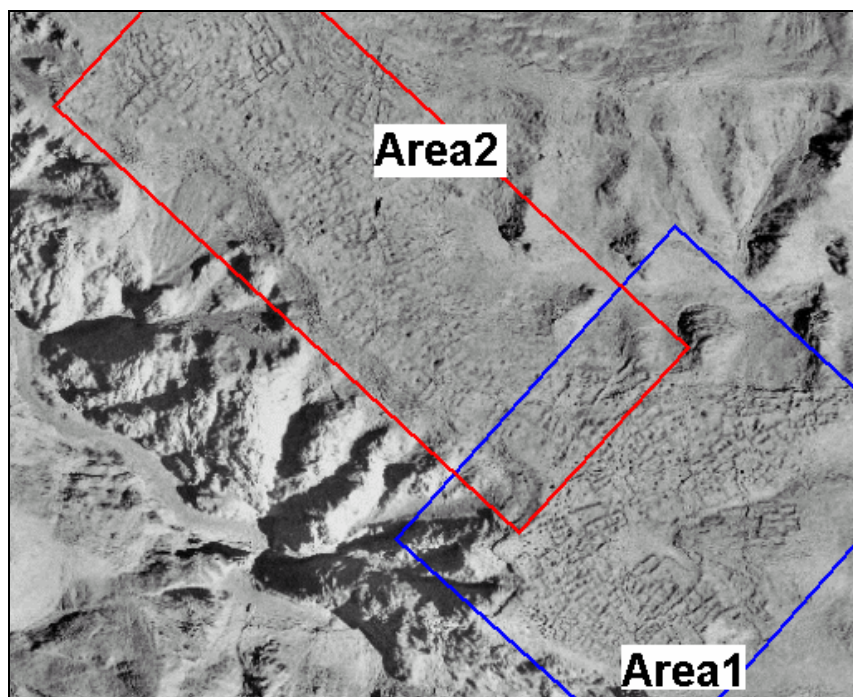


Figure 4. Area1 and Area2.

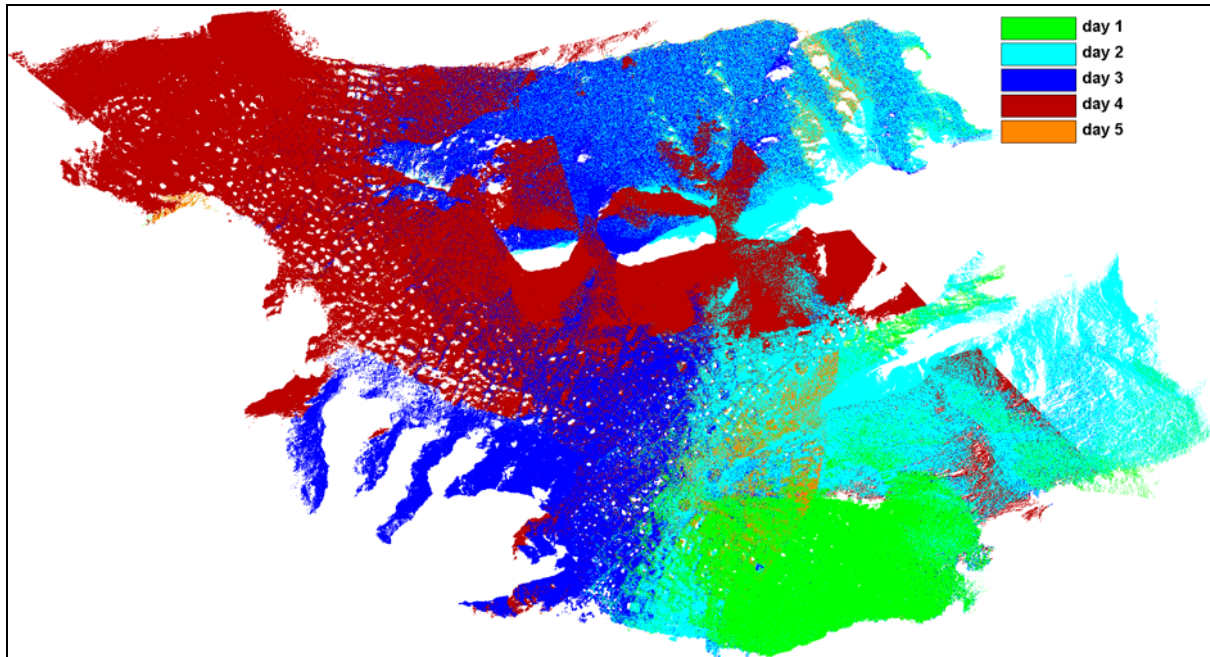


Figure 5. Day by day coverage of the site.

The area of the well preserved walls (Area1 in Fig. 4) was scanned in the first 3 days. In the continuing 4<sup>th</sup> and 5<sup>th</sup> days the Area2 was scanned with a lower point density level. Totally 144 million of points acquired in 57 scan files. Figure 5 shows the day by day coverage of the site. The point spacing is between 1-35 cm, changing with the range.

### 3.3. Pairwise registration with the LS3D surface matcher

The Pinchango Alto laser data set is a good example of large volume data sets with 144 million points from 57 stand points. Only the raw XYZ files in ASCII format occupy 3.83 GB memory area on a hard disk. Owing to our efficient boxing structure the large data size is not a problem at the registration phase from the data management and processing time point of views. However we faced with many limitations at the modeling phase, which will be explained in the fourth section.

Due to the topography of the site and relatively large incident angles of the signal paths large occlusions occurred in the point clouds (Fig. 6 and 7). This is a difficult case for the surface registration problem. However our surface matching algorithm LS3D successfully handled this problem.

Totally 130 consecutive matching processes were performed using the LS3D matching method. The matching 01-19 were done on an Intel® P4 2.53 GHz PC, and the rest 20-130 were done on an Intel® P4 3.40 GHz PC. All experiments were carried out using own self-developed C/C++ software. Since there was no scale difference between the scans, the scale factor  $m$  was fixed to unity by infinite weight value ( $(\mathbf{P}_b)_{ii} \rightarrow \infty$ ). The iteration criteria values  $c_i$  were selected as 1 mm for the translation vector and  $10^{cc}$  for the rotation angles.

All the LS3D matching processes were performed in the mono-patch mode. The multi-subpatch mode was not chosen, since interactively selecting of the subpatches is difficult due to low texture property of the site.

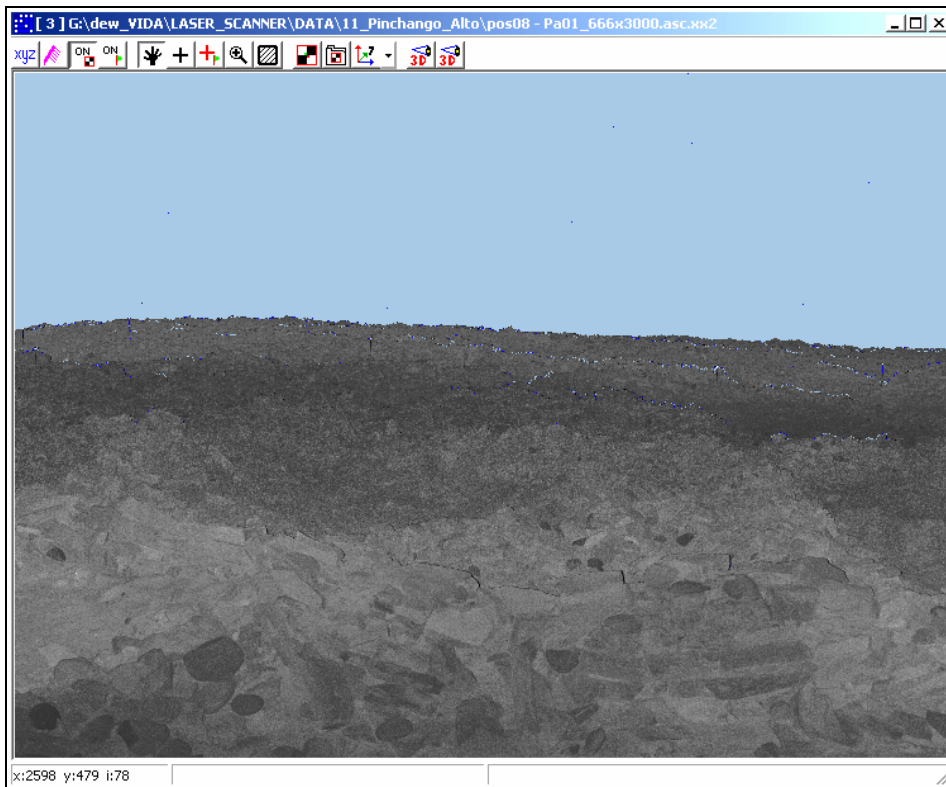


Figure 6. Intensity image of a nearly 90 degree subpart of scan #8.



Figure 7. Top view of the point cloud of Figure 6 in 3D.

In all experiments the initial approximations of the unknowns were provided by interactively selecting 3 common points on both surfaces before matching. If a common object, e.g. a stone, cannot be found on both surfaces, which is a common case due to low textural information of the area and large occlusions, the retro-reflective targets of the scanner were also used.

The numerical results of the LS3D matching processes are given in Table 1. In all case it successfully found the solution. No divergence or failure case occurred. The average sigma naught value is around 1.0 cm, which confirms the reported accuracy potential of the LMS-Z420i scanner.

As shown in Table 1 our proposed method provided successful matching results in reasonable processing times. Only during the matching of any pair of those three overview scans #01, #56 and #57 the computation times were relatively long, especially for the matching NO 116 (matching of scan #56 to scan #57 in Table 1). One reason is the extremely high number of points, i.e. matching of 2.7 million points to 3.2 million points requires heavy computation for the correspondence searching. Secondly scan #56, which the boxing structure was established for in matching NO 116, covers a large area of 230 x 350 meters in dimension. This requires a large number of cuboid elements in the boxing structure. But it was only possible to establish the boxing structure with 1200 x 1200 x 1200 elements due to the physical memory limit of the PC.

### 3.4. Global registration

The first scan (#01) was selected as the reference, which defines the datum of the common coordinate system. Since multiple overlaps exist among the point clouds, there is need for a global registration, which distributes the residuals evenly among all the scans, and also considers the closure condition, i.e. matching of the last scan to the first one. For this purpose we used the block adjustment by independent models solution, which was formerly proposed for global registration of laser scanner point clouds, but for the case of retro-reflective targets as tie points (Scaioni and Forlani, 2003).

In the LS3D matching processes, the final correspondences were saved to separate files. The number of tie points was thinned out by selecting of every 10<sup>th</sup> correspondence. Then all these files were given as input to the block adjustment by independent models software BAM7, which is an in-house software based on a 7-parameter 3D similarity transformation. It was run in the rigid body transformation mode by fixing the scale factor to unity. The block adjustment concluded with 0.5 cm *a posteriori* sigma value in 4 iterations. Decomposition of the sigma value into the main coordinate axes gives 0.3 cm, 0.3 cm, and 0.4 cm along *x-y-z* axes respectively. Those relatively homogeneous and small values show the success of the final agreement of all the point clouds.

## 4. Surface Mesh Generation and Modeling

After the registration all scan files were merged as one XYZ file, discarding the no data or the scanner signed erroneous points, e.g. scan points on the sky. This file totally contains 78.1 million points. It was further cropped to contain only the area of interest, finally with 69.2 million points. Two different commercial software packages were used for the modeling: Geomagic Studio 6 (Raindrop Geomagic) and ArcGIS 9 (ESRI). Both of the software run on an Intel® P4 3.40 GHz PC with 2 GB RAM.

Table 1. Numerical results of the LS3D matching.

NO	TMP scan no (#)	SRC scan no (#)	No. of TMP points (K)	No. of SRC points (K)	No. of COR points (K)	Iter.	Time (sec.)	Sigma naught (cm)	NO	TMP scan no (#)	SRC scan no (#)	No. of TMP points (K)	No. of SRC points (K)	No. of COR points (K)	Iter.	Time (sec.)	Sigma naught (cm)
1	01	02	2063	1132	502	9	98	1.9	66	36	37	825	923	106	7	37	1.1
2	02	03	1132	1101	731	8	77	1.0	67	37	38	923	829	219	12	49	1.2
3	03	04	1101	1099	531	6	55	0.9	68	38	39	829	875	166	11	50	1.0
4	04	05	1099	1072	631	7	111	0.7	69	39	40	875	874	69	8	24	1.3
5	05	06	1072	1068	841	6	264	0.8	70	40	41	874	860	204	10	53	1.0
6	06	07	1068	1060	789	8	139	1.0	71	41	42	860	886	283	9	86	0.9
7	07	08	1060	1059	738	8	152	1.6	72	42	43	886	788	363	8	78	1.2
8	08	09	1037	1096	556	8	90	2.8	73	43	44	788	737	163	12	42	1.1
9	09	10	1096	1023	292	8	40	2.5	74	44	45	737	826	54	12	22	1.0
10	10	11	1023	1006	613	9	113	1.5	75	45	46	826	851	108	10	34	0.9
11	11	12	1006	980	693	8	260	2.0	76	46	47	851	830	348	8	91	0.8
12	01	03	1926	1085	337	10	58	1.5	77	16	30	819	766	360	8	169	0.8
13	01	05	1926	1045	104	8	37	1.2	78	16	31	819	892	248	6	74	1.2
14	01	07	1926	1037	232	9	47	1.7	79	30	31	766	892	95	6	36	1.2
15	01	09	1926	1096	367	8	119	1.4	80	18	32	937	907	260	8	86	1.0
16	03	09	1085	1096	99	7	25	1.0	81	18	31	937	892	97	10	44	1.1
17	04	07	1077	1037	383	5	61	0.7	82	19	33	967	931	296	6	84	0.6
18	04	06	1077	1043	413	6	59	0.7	83	19	32	967	907	148	8	58	0.6
19	07	12	1037	980	455	11	69	1.6	84	20	33	986	931	221	6	41	1.0
20	12	13	980	939	298	8	85	1.1	85	20	34	986	923	237	7	43	1.0
21	13	14	939	810	359	11	97	1.2	86	21	34	970	923	338	5	54	1.0
22	14	15	810	792	309	11	129	0.9	87	21	35	970	871	135	9	41	0.9
23	15	16	792	819	357	9	186	0.9	88	22	35	924	871	180	6	33	1.0
24	16	17	819	939	220	9	108	1.1	89	22	36	924	825	153	6	29	1.1
25	17	18	939	937	364	8	73	1.3	90	23	36	819	825	79	5	21	1.1
26	18	19	937	967	285	10	66	1.2	91	35	38	871	829	81	7	30	1.1
27	19	20	967	986	303	8	65	0.7	92	34	39	923	875	172	6	53	0.9
28	20	21	986	970	421	10	70	1.1	93	35	39	871	875	90	7	33	1.0
29	21	22	970	924	243	10	59	1.2	94	33	39	931	875	69	10	35	1.1
30	22	23	924	819	270	10	49	1.3	95	32	42	907	886	140	11	81	0.9
31	23	24	819	840	316	5	46	1.3	96	31	42	892	886	107	10	50	1.0
32	24	25	840	926	166	8	44	1.1	97	31	43	892	788	64	15	39	1.0
33	25	26	926	1028	291	10	72	1.2	98	41	43	860	788	148	9	47	0.8
34	26	27	1028	1073	313	11	76	1.1	99	41	44	860	737	184	8	48	0.8
35	27	28	1073	899	521	6	75	1.0	100	40	45	874	826	314	7	133	0.6
36	28	29	899	832	253	7	64	1.3	101	40	46	874	851	78	8	32	0.8
37	07	11	1037	1006	139	10	45	0.9	102	39	46	875	851	231	9	170	0.6
38	09	11	1096	1006	160	7	26	1.3	103	38	46	829	851	86	8	54	0.6
39	08	11	1037	1006	180	10	52	1.6	104	38	47	829	830	174	6	60	0.7
40	07	13	1037	939	150	9	31	1.1	105	41	45	860	826	71	8	29	0.8
41	06	13	1043	939	155	8	37	0.8	106	37	50	923	2349	26	8	14	1.1
42	05	13	1045	939	176	8	39	0.8	107	50	49	2349	3142	332	5	64	0.9
43	14	16	810	819	218	10	58	1.0	108	49	48	3142	2221	238	7	58	0.9
44	13	16	939	819	285	10	55	1.1	109	50	51	2349	3167	74	6	25	0.9
45	13	17	939	939	328	8	87	1.0	110	49	51	3142	3167	45	5	21	0.9
46	12	17	980	939	270	8	68	1.3	111	48	52	2221	2676	91	15	38	0.6
47	11	18	1006	937	381	10	77	1.2	112	52	53	2676	3178	563	10	290	0.8
48	10	19	1023	967	278	6	48	0.8	113	53	54	3178	2457	169	18	98	0.8
49	10	20	1023	986	135	6	21	1.0	114	54	55	2457	3147	41	10	29	1.0
50	01	20	1926	986	67	7	24	1.0	115	01	57	1926	3250	499	7	574	0.5
51	01	26	1926	1028	98	8	46	1.0	116	57	56	3250	2703	926	3	1353	0.3
52	01	27	1926	1073	102	7	36	1.0	117	37	51	923	3167	382	4	45	1.2
53	22	25	924	926	170	6	36	1.1	118	36	51	825	3167	196	5	35	1.2
54	24	29	840	832	111	5	19	1.2	119	23	51	819	3167	200	6	37	1.2
55	24	28	840	899	146	4	31	1.0	120	38	51	829	3167	147	5	30	1.2
56	25	28	926	899	205	6	35	1.3	121	47	50	830	2349	157	5	28	1.2
57	26	28	1028	899	176	9	31	1.3	122	37	49	923	3142	91	5	29	1.3
58	21	26	970	1028	53	9	22	1.0	123	20	56	986	2703	262	12	48	0.8
59	15	30	792	766	420	11	190	0.9	124	10	56	1023	2703	227	11	55	0.6
60	17	31	939	892	292	10	81	1.1	125	09	56	1096	2703	547	10	81	0.6
61	31	32	892	907	192	10	49	1.2	126	21	56	970	2703	166	13	45	0.7
62	32	33	907	931	188	9	38	1.3	127	21	57	970	3250	236	13	60	0.7
63	33	34	931	923	134	9	38	1.1	128	20	57	986	3250	238	11	47	0.7
64	34	35	923	871	347	6	72	1.1	129	19	57	967	3250	79	10	35	0.5
65	35	36	871	825	172	9	39	1.3	130	01	56	1926	2703	631	3	432	0.6

NO : Matching 01-19 were done on an Intel® P4 2.53 GHz PC, and the rest 20-130 were done on an Intel® P4 3.40 GHz PC

TMP : Template surface, SRC: search surface, COR: corresponding.

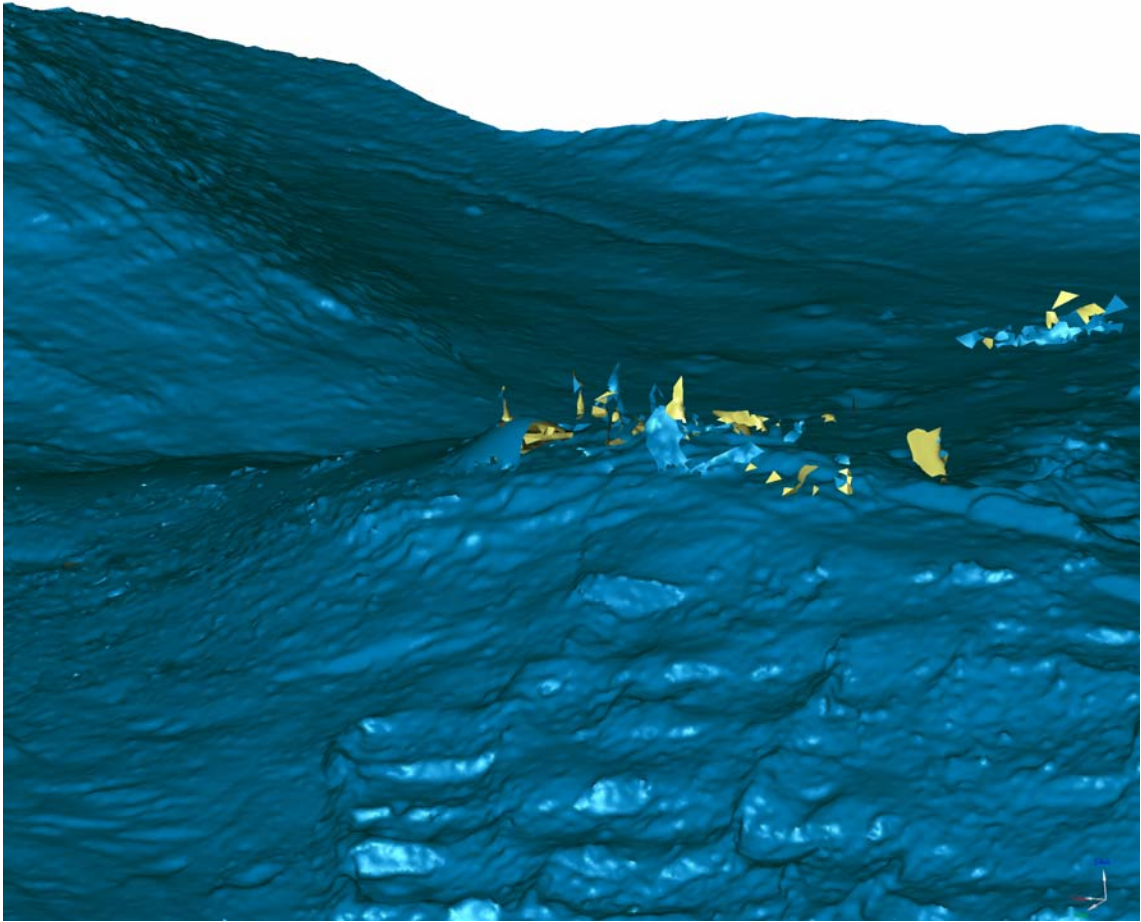


Figure 8. Non-static objects on the site.

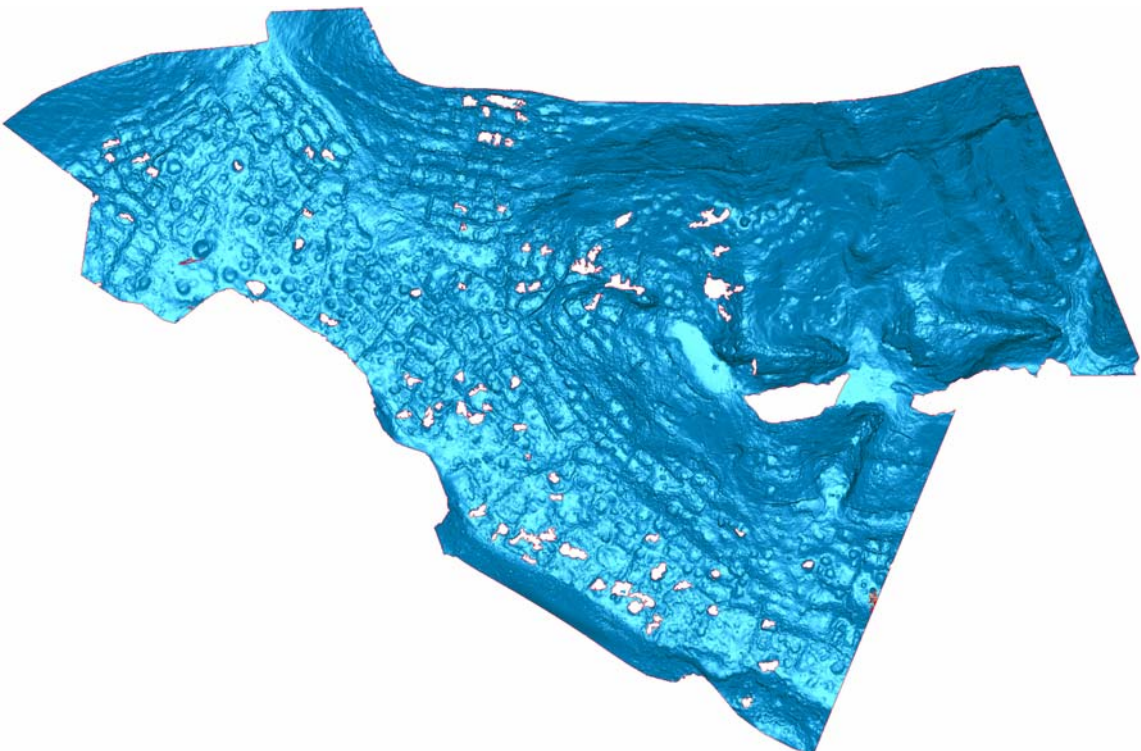


Figure 9. Holes due to missing data.

#### 4.1. Modeling with Geomagic Studio 6

As a first attempt the mesh generation was tried at the original data resolution with 69.2 million points. The software recommended setting the target number of triangles to 2.5 millions, which is clearly suboptimal. When this recommendation is ignored, the operation could not be performed, since the memory request of the software exceeded the physical memory limit 2 GB of the computer.

The number of points was reduced to 14.8 million point using the “grid sampling” function with a 5 cm grid size. Then the point cloud file was split to two files to overcome of memory limitation. This was done manually, since the software does not provide any automatic solution. Finally surface wrapping was done for both parts separately with a medium level noise reduction option.

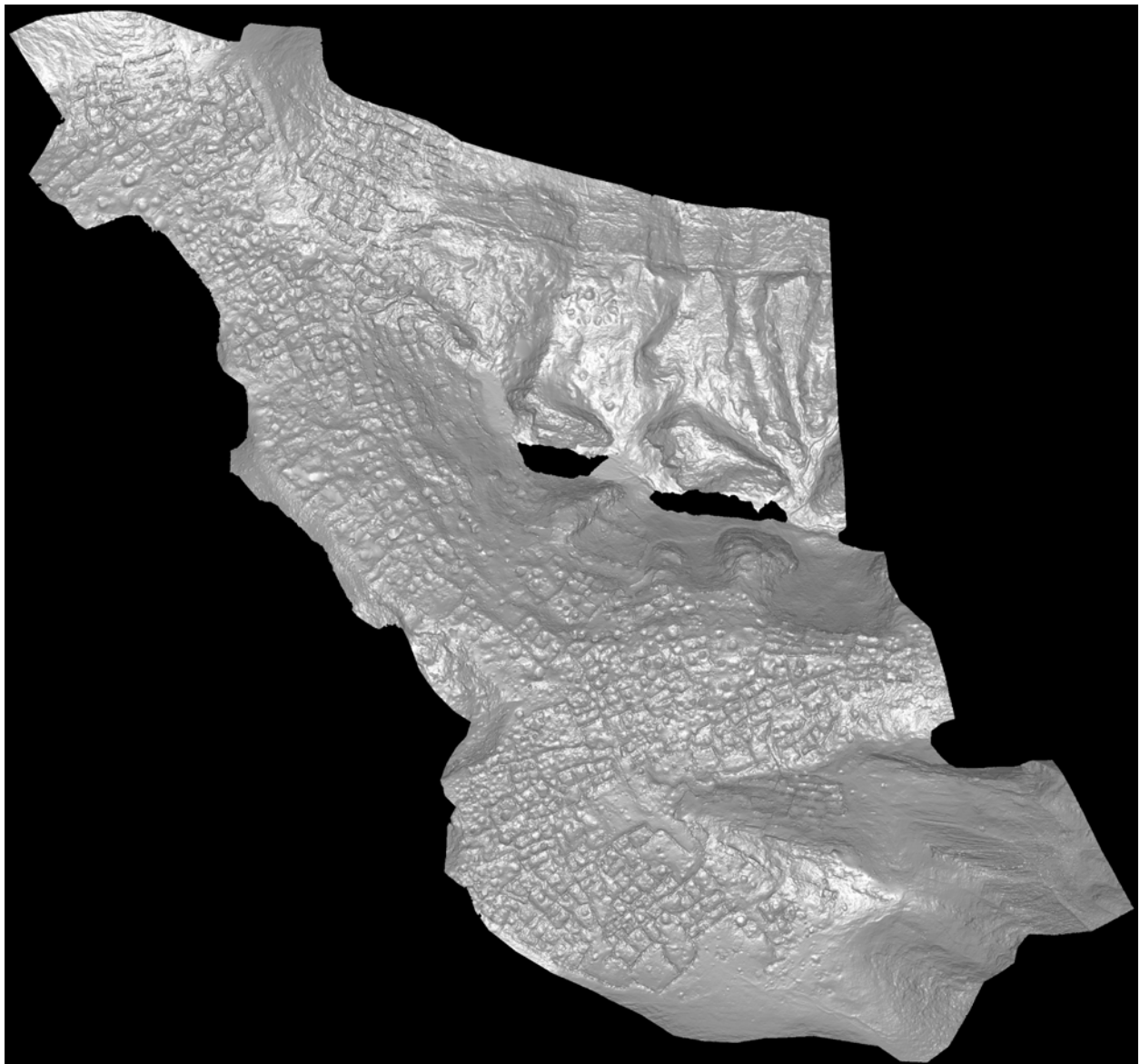


Figure 10. Shaded view of the generated model using Geomagic Studio 6.

All the displaced objects during the 5 days fieldwork, e.g. people, GPS, helicopter, bags, boxes, etc., produced errors in the generated mesh (Fig. 8). Those errors were edited manually. Because of data unavailability some holes occurred on the meshed surface

(Fig. 9). Missing data parts are usually due to occlusions of walls and the hollows. They were filled with the “Fill Holes” function of the software.

After the editing step those two meshed surface parts were merged as one manifold. The final model contains 5.8 million triangles (Fig. 10).

#### 4.2. Modeling with ArcGIS 9

3D Analyst extension under the module ArcMap was used for the surface interpolation. The ArcMap was not able to load the data at the original resolution. After testing with the several numbers of points, it could load and process the point cloud with 5.2 million points. Reducing the number of points was carried out again using the “grid sampling” function of Geomagic Studio with a 10 cm grid size.

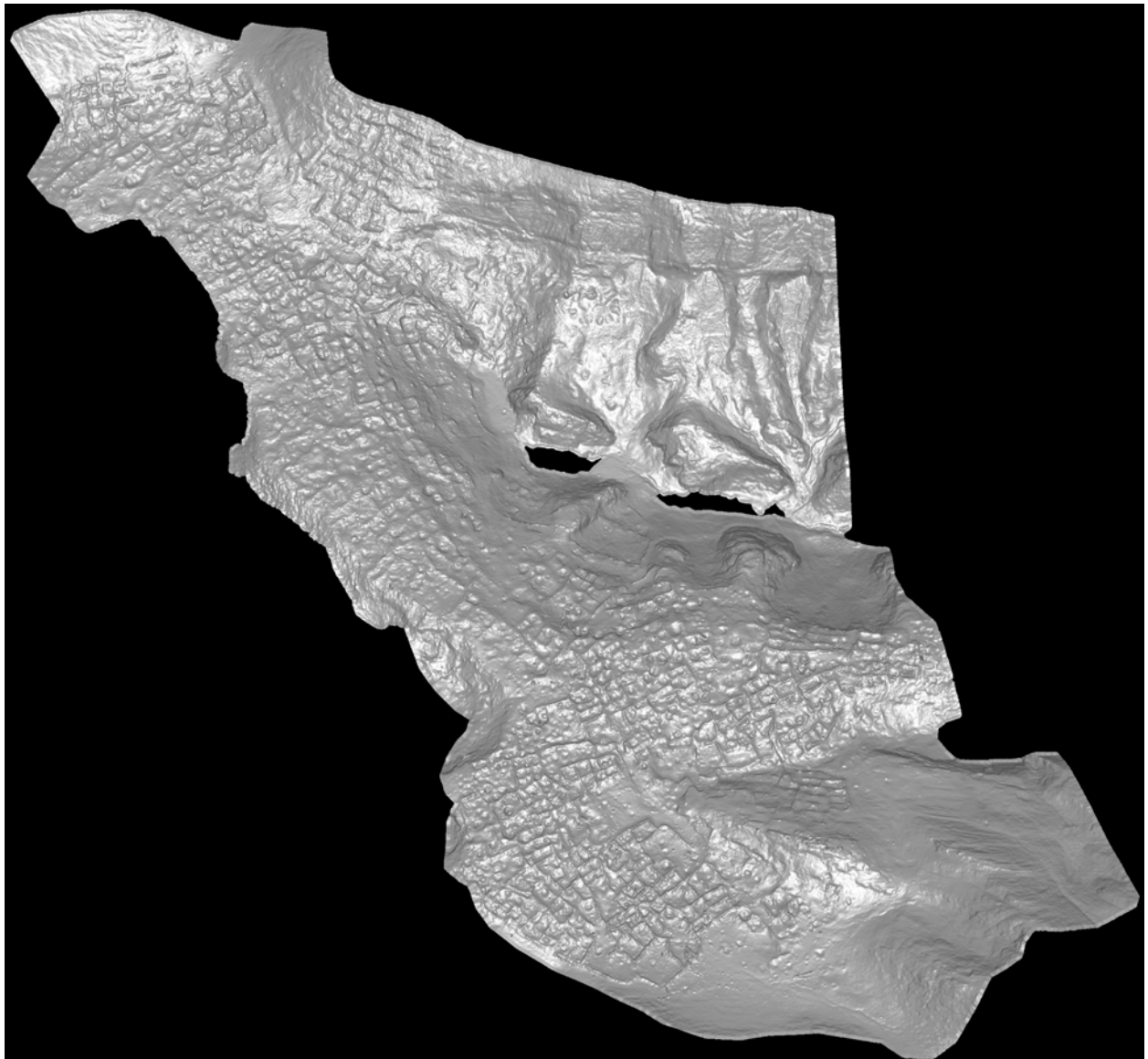


Figure 11. Shaded view of the generated model using ArcGIS 9.

The point cloud was interpolated to regular grid form using the “Inverse Distance Weighted” option of the 3D Analyst. The artifacts due to moving objects were edited.

Other than in Geomagic Studio, all missing data parts were automatically interpolated. The final model contains 5.0 million triangles (Fig. 11).

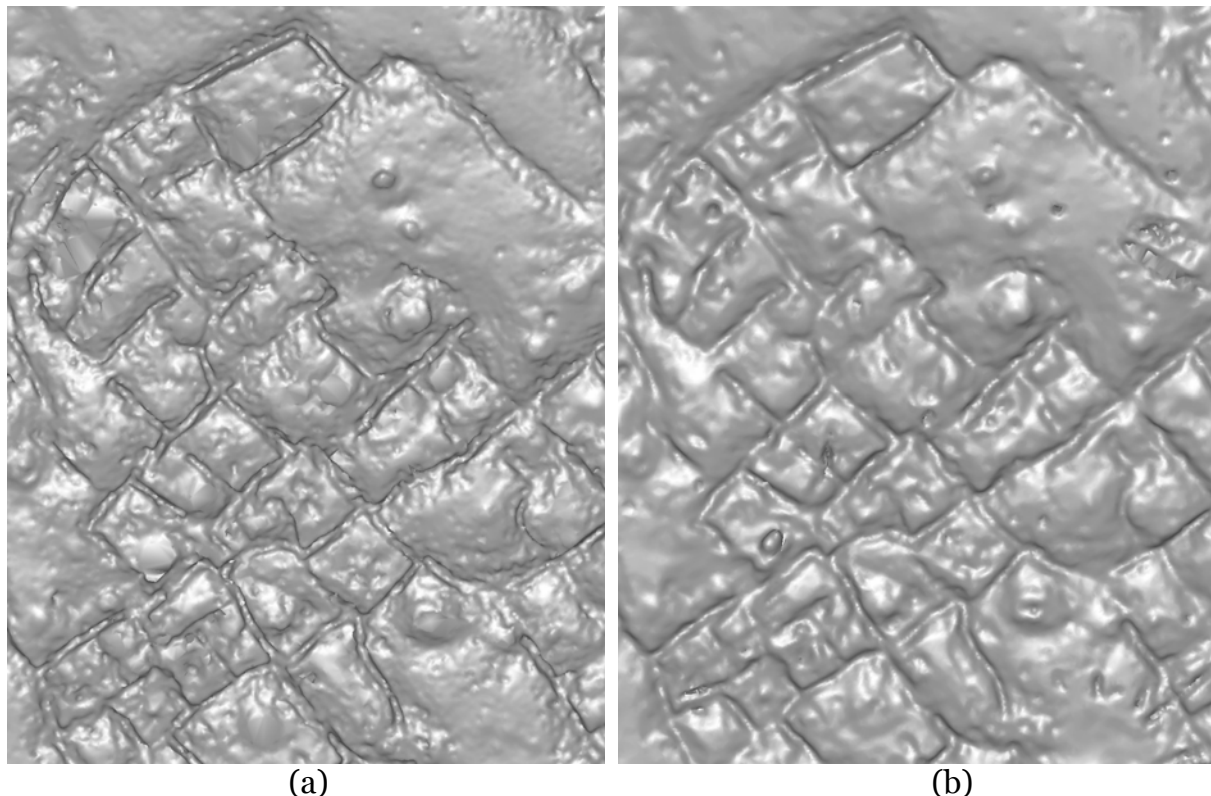


Figure 12. The same zoom in area of the generated surface model using Geomagic Studio (a) and ArcGIS (b).

The ArcGIS apparently generates the smoother model because of two reasons (Fig. 12). Firstly, it is a 2.5D modeling software, which is not optimal for real 3D objects. Geomagic Studio is a real 3D modeling software. Secondly, ArcGIS used much less points than Geomagic Studio for the mesh generation.

## 5. Conclusions

The disadvantages of the target based registration of the laser scanning point clouds are well known. Adopting a target based registration approach requires more fieldwork and personnel, i.e. setting up those targets to the site and measuring them using a theodolite or a GPS system. It is apparent that additional geodetic measurement devices increase the equipment cost as well. The target based registration methods cannot exploit the full accuracy potential of the data, due to additional errors introduced by the geodetic measurements. Although the laser data naturally has very high level of redundancy, the target based registration techniques use only a very small portion of the data. This is the second reason causing to degrade the accuracy potential.

Surface based registration techniques stand as efficient and versatile alternative to the target based techniques. They offer better registration results while keeping the project cost lower.

In this study we showed the capabilities our surface based registration method applying to the Pinchango Alto laser scanning data set. Our proposed method, the Least Squares

3D Surface Matching (LS3D), estimates the transformation parameters between two or more fully 3D surfaces, using the Generalized Gauss Markoff model, minimizing the sum of squares of the Euclidean distances between the surfaces. The mathematical model is a generalization of the least squares image matching method and offers high flexibility for any kind of 3D surface correspondence problem. The least squares concept allows for the monitoring of the quality of the final results by means of precision and reliability criterions.

The Pinchango Alto data set stands as a special case due to the huge volume and many occlusions on the data. The practical example shows that our proposed method can provide successful matching results in reasonable processing times. It exploits the full accuracy potential of the data owing to its powerful mathematical model.

The following up step surface modeling was performed by use of commercial software packages. However, it was not possible to model in the original resolution. Due to not efficient memory management capabilities of the software packages, the modeling had to be performed at reduced resolution. The modeling of 3D laser scanner point clouds is still a troublesome step and sophisticated algorithms need to be developed with real 3D capabilities.

## Acknowledgements

The Pinchango Alto laser scanning data set was kindly provided by Riegl GmbH (Austria), which is gratefully acknowledged.

## References

- Akca, D., and Gruen, A., 2005. Fast correspondence search for 3D surface matching. To appear in: ISPRS Workshop "Laser Scanner 2005", Enschede, September 12-14.
- Chetverikov, D., 1991. Fast neighborhood search in planar point sets. *Pattern Recognition Letters*, 12(7), 409-412.
- Eisenbeiss, H., Lambers, K., and Sauerbier, M., 2005. Photogrammetric recording of the archaeological site of Pinchango Alto (Palpa, Peru) from a mini helicopter (UAV). In *Proc. Of the 33<sup>rd</sup> CAA Conference, Tomar, Portugal, March 21-24* (in press).
- Greaves, T., 2005. Laser scanning shaves weeks from failure analysis of parking garage collapse. *Spar View<sup>TM</sup>*, 3(14), <http://www.sparllc.com/archiveviewer.php?vol=03&num=14&file=vol03no14-01> (accessed August 2005).
- Gruen, A., 1985. Adaptive least squares correlation: a powerful image matching technique. *South African Journal of Photogrammetry, Remote Sensing and Cartography*, 14(3), 175-187.
- Gruen, A., Baltsavias, E.P., 1988. Geometrically constrained multiphoto matching. *Photogrammetric Engineering & Remote Sensing*, 54(5), 633-641.
- Gruen, A., and Akca, D., 2004. Least squares 3D surface matching. *International Archives of the Photogrammetry, Remote Sensing and Spatial Information Sciences*, 34(5/W16), (on CD-ROM).

- Gruen, A., and Akca, D., 2005a. Least squares 3D surface matching. ASPRS 2005 Annual Conference, Baltimore (Maryland), March 7-11 (on CD-ROM).
- Gruen, A., and Akca, D., 2005b. Least squares 3D surface and curve matching. ISPRS Journal of Photogrammetry & Remote Sensing, 59(3), 151-174.
- Pinchango Alto Project website, 2005.  
<http://www.photogrammetry.ethz.ch/research/pinchango> (accessed August 2005).
- Riegl Website, 2005. [http://www.riegl.co.at/terrestrial\\_scanners/lms-z420i\\_z420i\\_all.htm](http://www.riegl.co.at/terrestrial_scanners/lms-z420i_z420i_all.htm) (accessed August 2005).
- Scaioni, M., and Forlani, G., 2003. Independent model triangulation of terrestrial laser scanner data. International Archives of the Photogrammetry, Remote Sensing and Spatial Information Sciences, 34(5/W12), 308-313.
- Sternberg, H., Kersten, Th., Jahn, I., and Kinzel, R., 2004. Terrestrial 3D laser scanning – data acquisition and object modeling for industrial as-built documentation and architectural applications. International Archives of the Photogrammetry, Remote Sensing and Spatial Information Sciences, 35(B7), 942-947.